

Note to readers with disabilities: *EHP* strives to ensure that all journal content is accessible to all readers. However, some figures and Supplemental Material published in *EHP* articles may not conform to [508 standards](#) due to the complexity of the information being presented. If you need assistance accessing journal content, please contact ehp508@niehs.nih.gov. Our staff will work with you to assess and meet your accessibility needs within 3 working days.

Supplemental Material

Quality Control for Single Cell Imaging Analytics Using Endocrine Disruptor-Induced Changes in Estrogen Receptor Expression

Fabio Stossi, Pankaj K. Singh, Ragini M. Mistry, Hannah L. Johnson, Radhika D. Dandekar, Maureen G. Mancini, Adam T. Szafran, Arvind U. Rao, and Michael A. Mancini

Table of Contents

Figure S1. Additional quality control analysis and simulations. A) Principal Components Analysis (PCA) of the 31 replicate experiments in Figure 1C. B) simulation analysis showing the number of experiments needed to obtain a reliable reference distribution. C) simulations showing the minimum number of cells that need to be acquired in one experiment to have a reliable approximation of the reference distribution. D) Earth Mover's Distance (EMD) analysis of 28 replicated wells in the same 384 well plate to highlight well-to-well variation in Estrogen Receptor alpha (ER) distribution. Red dotted line (on right) corresponds to three standard deviations from the mean cluster (represented by the black dotted line on the left). E) EMD calculations comparing three different ER antibodies used simultaneously in a triple immunofluorescence assay in MCF-7 cells. Red dotted line corresponds to the reference distribution. Blue dotted line corresponds to 3 standard deviations away from the reference distribution. Summary tables for this figure are in Excel Table S18.

Figure S2. Raw data for the fold median Estrogen Receptor level descriptor in MCF-7 cells treated with the EPA45 compounds (Judson et al. 2015). Average and standard deviation of N=4 is graphed. Summary tables for this figure are in Excel Table S19.

Figure S3. Raw data for the fold quadratic entropy (QE) descriptor in MCF-7 cells treated with the EPA45 compounds. Average and standard deviation of N=4 is graphed. Summary tables for this figure are in Excel Table S19.

Figure S4. Raw data for the Earth Mover's Distance (EMD) descriptor in MCF-7 cells treated with the EPA45 compounds. Average and standard deviation of N=4 is graphed. Summary tables for this figure are in Excel Table S19.

Figure S5. Comparison between three independent batches of the EPA45 compounds obtained from the EPA. A) Pairwise Pearson's correlation hierarchical clustering for the EPA45 chemicals comparing the effects of each compound on Estrogen Receptor (ER) levels measured by immunofluorescence across three batches of chemicals obtained from the EPA over time. Experimental setting (time treatment and concentration ranges are the same as in Figure 4). ER nuclear levels represent here the Fold Median for ER levels compared to DMSO vehicle samples. B) example of chemicals that showed batch-to-batch variation. Summary tables for this figure are in Excel Table S20.

Figure S6. Raw data for the fold media descriptor in MCF-7 cells treated with the ATSDR42 compounds. Average and standard deviation of N=4 is graphed. Summary tables for this figure are in Excel Table S21.

Figure S7. Raw data for the fold quadratic entropy (QE) descriptor in MCF-7 cells treated with the ATSD42 compounds. Average and standard deviation of N=4 is graphed. Summary tables for this figure are in Excel Table S21.

Figure S8. Raw data for the Earth Mover's Distance (EMD) descriptor in MCF-7 cells treated with the ATSDR42 compounds. Average and standard deviation of N=4 is graphed. Summary tables for this figure are in Excel Table S21.

Figure S9. Validation of anti-ER α Clone 127 antibody. An engineered GFP-ER:PRL-HeLa cell line (Ashcroft FJ et al., Gene 2011), that stably expresses GFP-tagged ER α , was treated with 10 nM E2 for 1 hour. Cells were immunolabeled with anti-ER α clone 127 antibody and visualized using an anti-Mouse IgG AlexaFluor 647 secondary. Samples were imaged at 20x/0.75 using an IC200 image cytometer (Vala Sciences). Representative fields of (A) GFP-ER α and (B) anti-ER α clone 127 labeling is shown along with the (C) merged image. Nuclear regions were determined (blue lines) using DAPI staining and nuclear GFP and antibody signal intensity extracted. (D) A scatterplot comparing single-cell nuclear GFP-ER α and anti-ER α intensity was generated using > 1450 cells. A Pearson's correlation analysis (red line) indicates high correlation (0.97) between the two signals. (E) Representative single cell GFP-ER α , anti-ER α , and merged images are shown which display a high correlation between signals at the sub-nuclear level. (F) Western blot analysis of whole MCF-7 cell lysates probed using anti-ER α clone 127 and anti-ER α clone 60C (Millipore 04-820).

References

Additional File- Excel Document

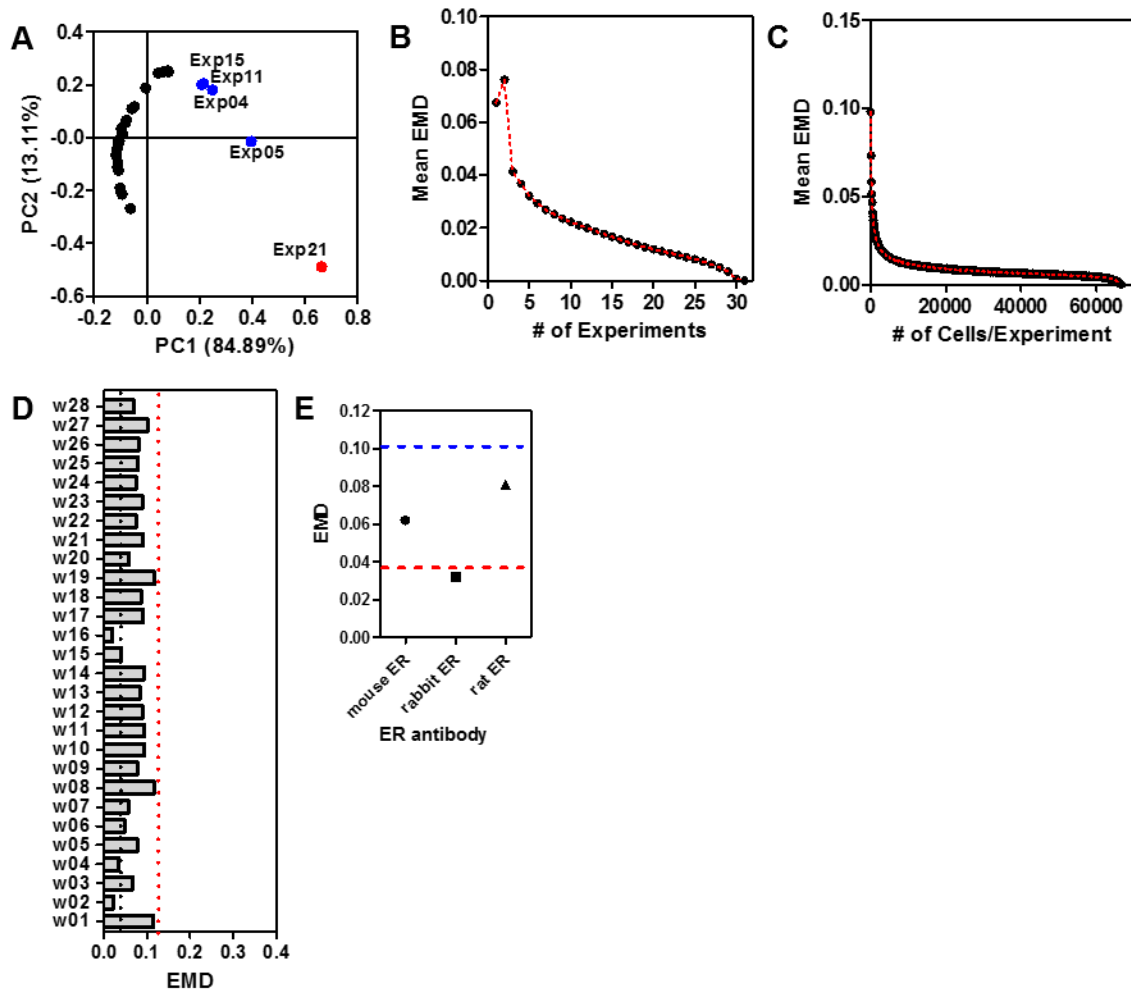


Figure S1. Additional quality control analysis and simulations. A) Principal Components Analysis (PCA) of the 31 replicate experiments in Figure 1C. B) simulation analysis showing the number of experiments needed to obtain a reliable reference distribution. C) simulations showing the minimum number of cells that need to be acquired in one experiment to have a reliable approximation of the reference distribution. D) Earth Mover's Distance (EMD) analysis of 28 replicated wells in the same 384 well plate to highlight well-to-well variation in Estrogen Receptor alpha (ER) distribution. Red dotted line (on right) corresponds to three standard deviations from the mean cluster (represented by the black dotted line on the left). E) EMD calculations comparing three different ER antibodies used simultaneously in a triple immunofluorescence assay in MCF-7 cells. Red dotted line corresponds to the reference distribution. Blue dotted line corresponds to 3 standard deviations away from the reference distribution. Summary tables for this figure are in Excel Table S18.

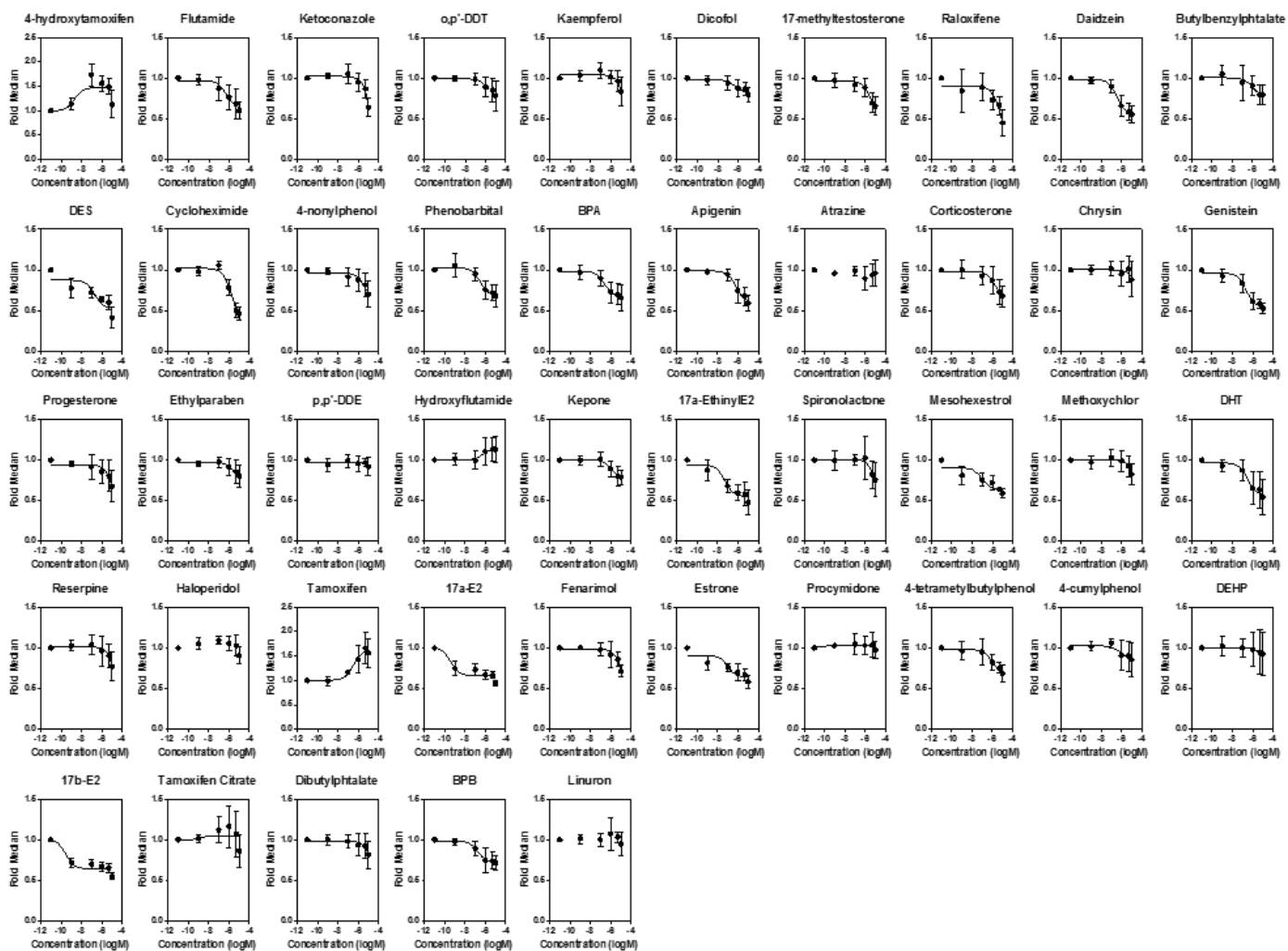


Figure S2. Raw data for the fold median Estrogen Receptor level descriptor in MCF-7 cells treated with the EPA45 compounds (Judson et al. 2015). Average and standard deviation of N=4 is graphed. Summary tables for this figure are in Excel Table S19.

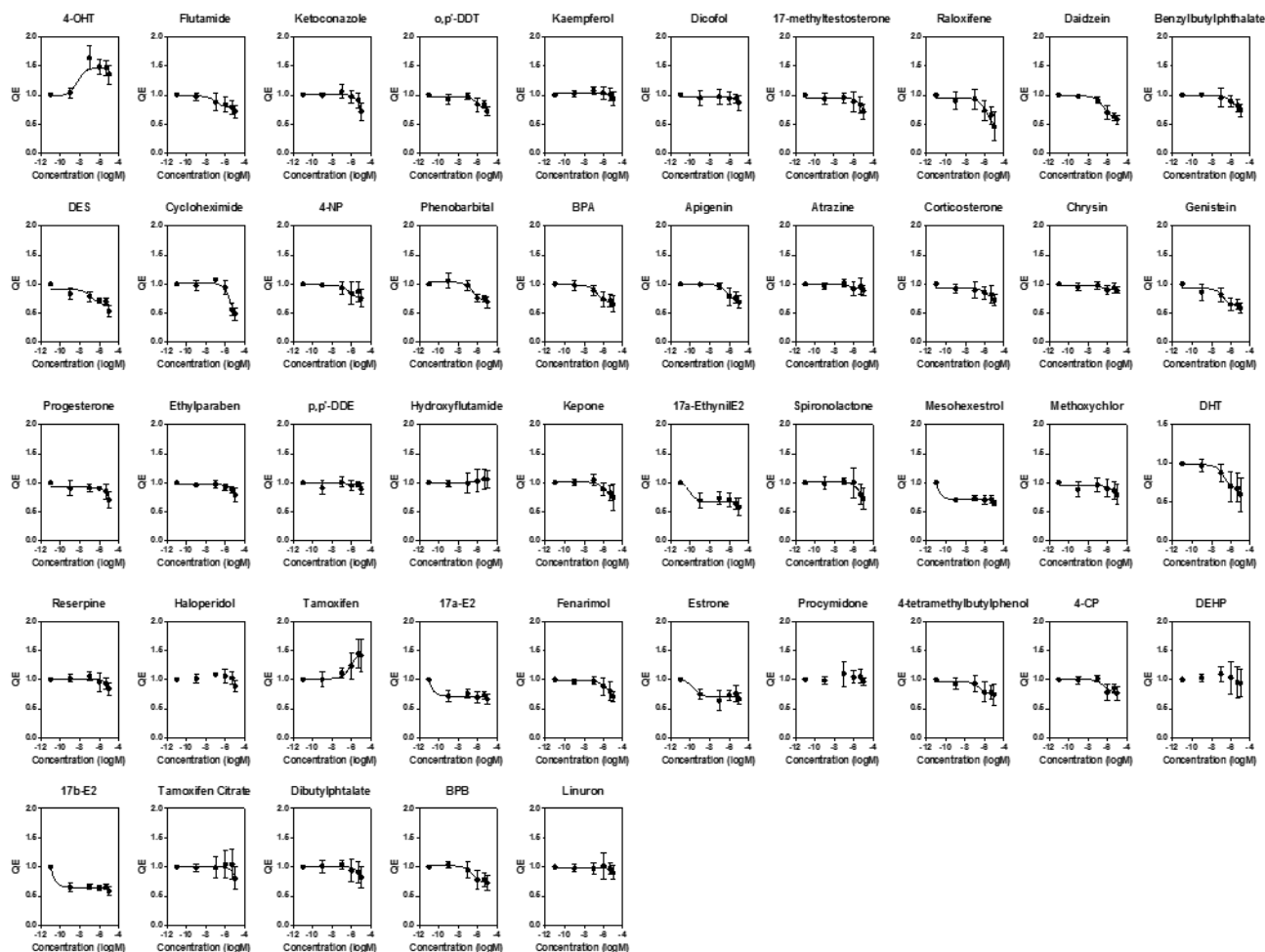


Figure S3. Raw data for the fold quadratic entropy (QE) descriptor in MCF-7 cells treated with the EPA45 compounds. Average and standard deviation of N=4 is graphed. Summary tables for this figure are in Excel Table S19.

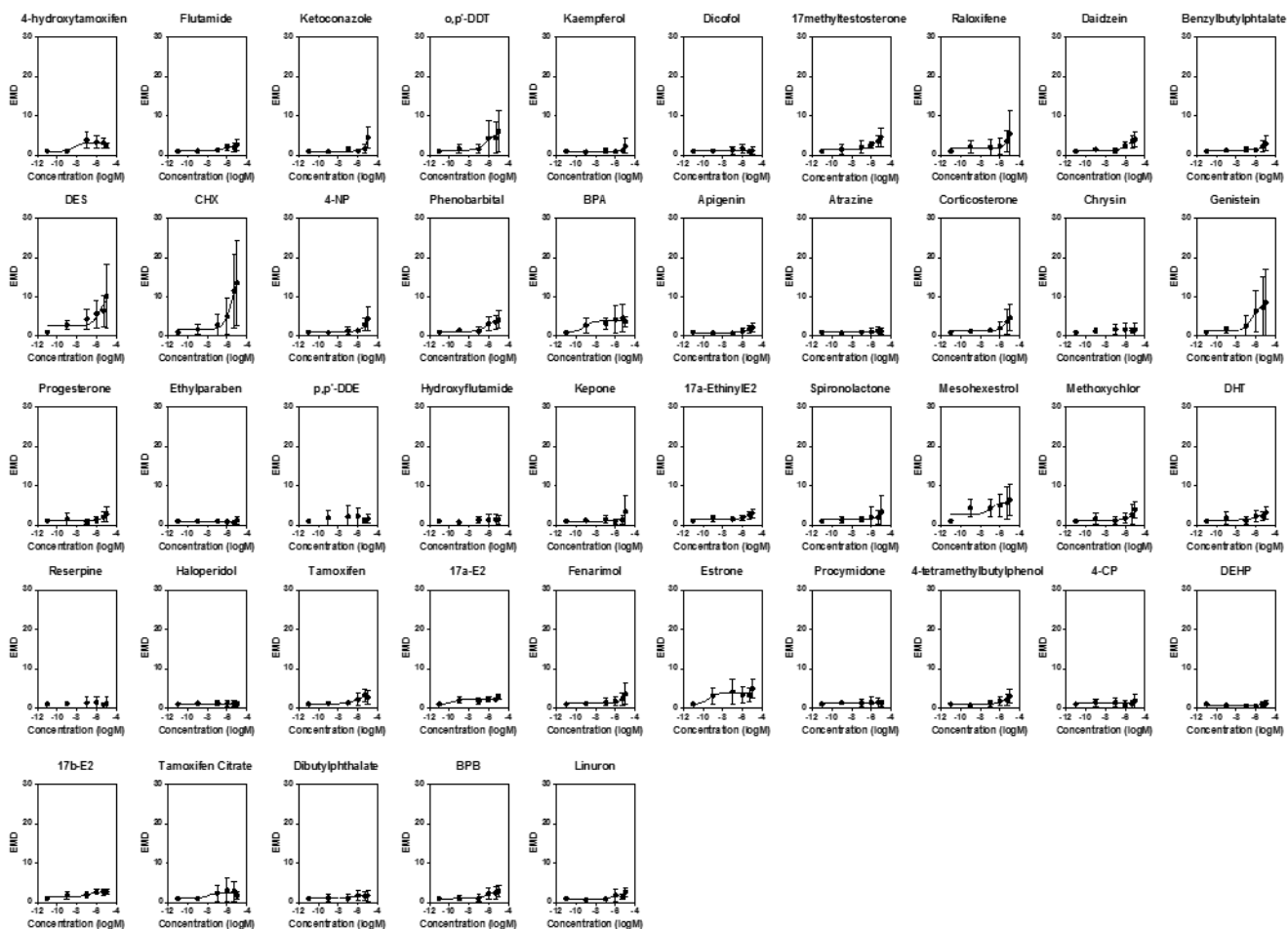


Figure S4. Raw data for the Earth Mover's Distance (EMD) descriptor in MCF-7 cells treated with the EPA45 compounds. Average and standard deviation of N=4 is graphed. Summary tables for this figure are in Excel Table S19.

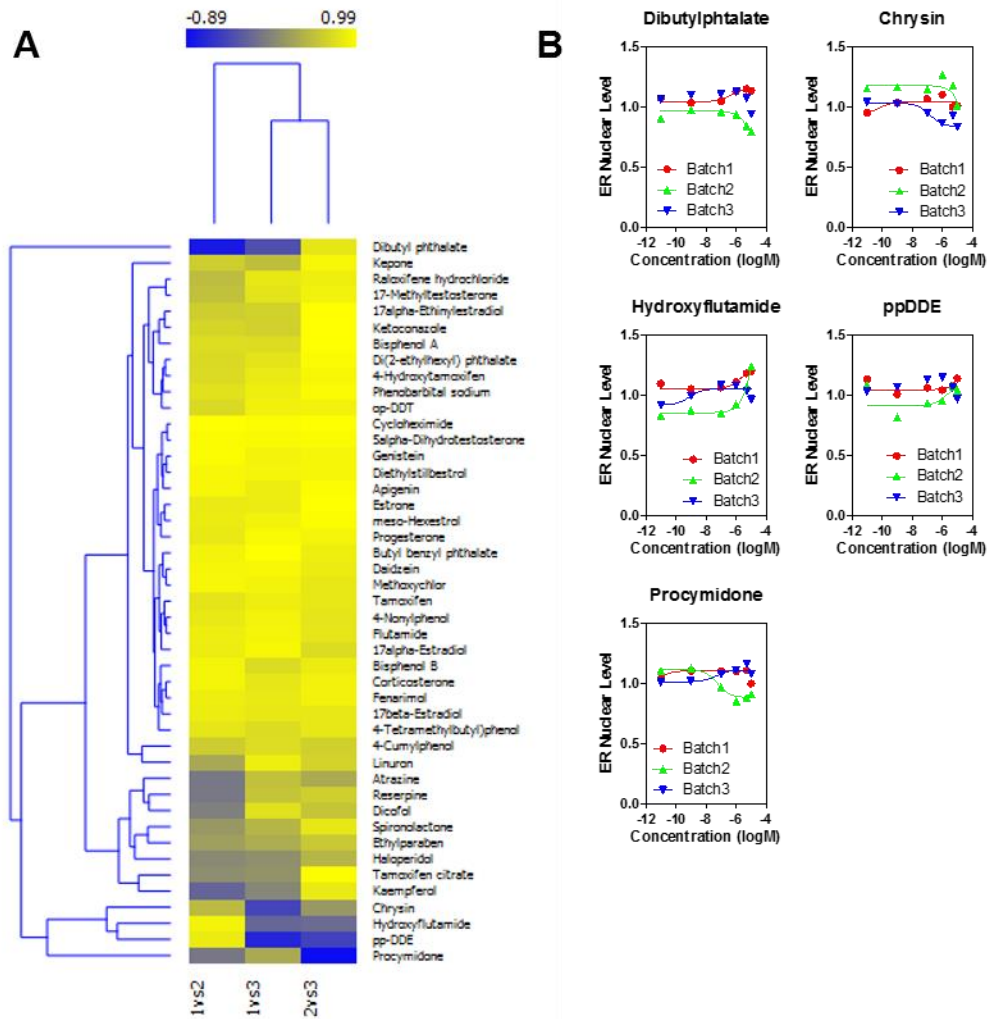


Figure S5. Comparison between three independent batches of the EPA45 compounds obtained from the EPA. A) Pairwise Pearson's correlation hierarchical clustering for the EPA45 chemicals comparing the effects of each compound on Estrogen Receptor (ER) levels measured by immunofluorescence across three batches of chemicals obtained from the EPA over time. Experimental setting (time treatment and concentration ranges are the same as in Figure 4). ER nuclear levels represent here the Fold Median for ER levels compared to DMSO vehicle samples. B) example of chemicals that showed batch-to-batch variation. Summary tables for this figure are in Excel Table S20.

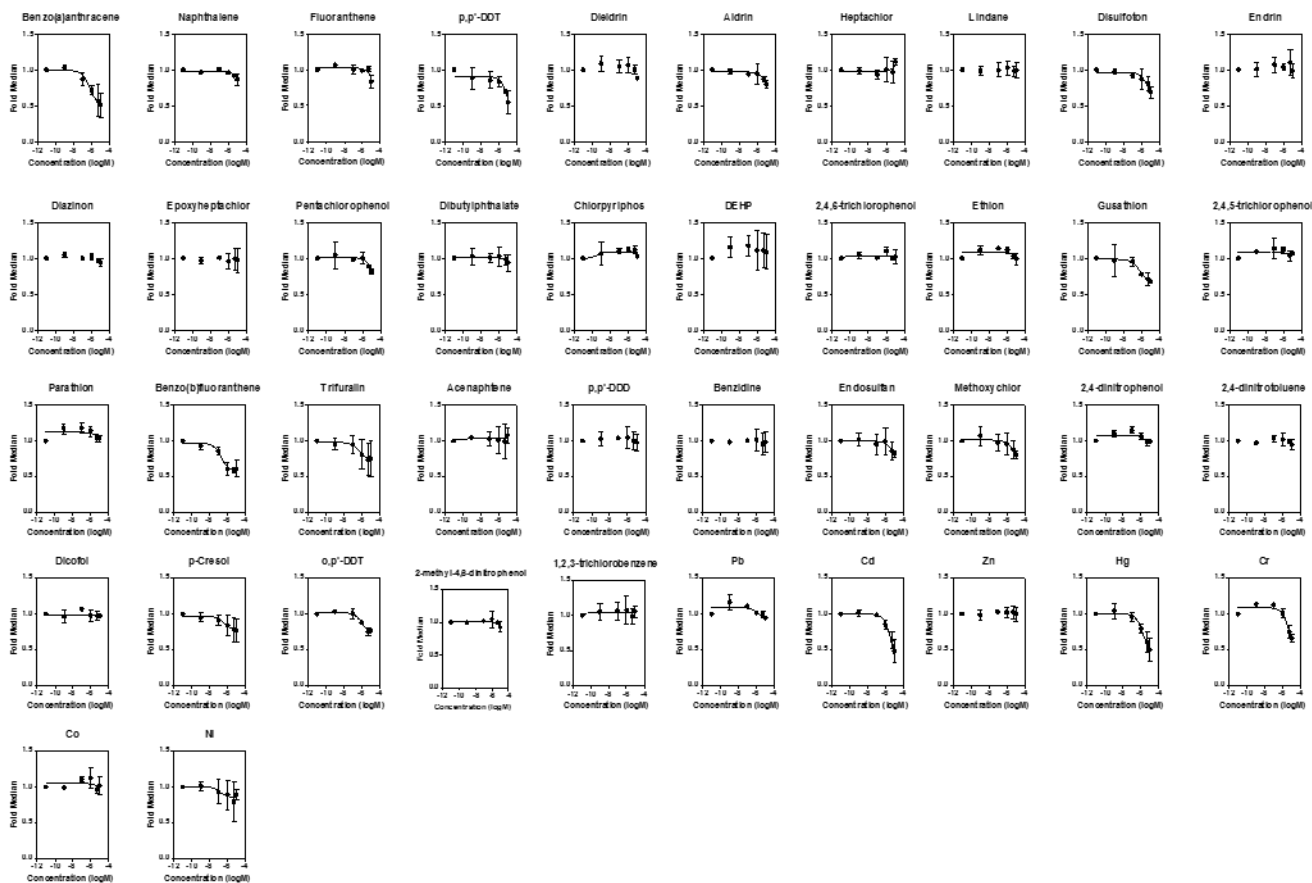


Figure S6. Raw data for the fold media descriptor in MCF-7 cells treated with the ATSDR42 compounds. Average and standard deviation of N=4 is graphed. Summary tables for this figure are in Excel Table S21.

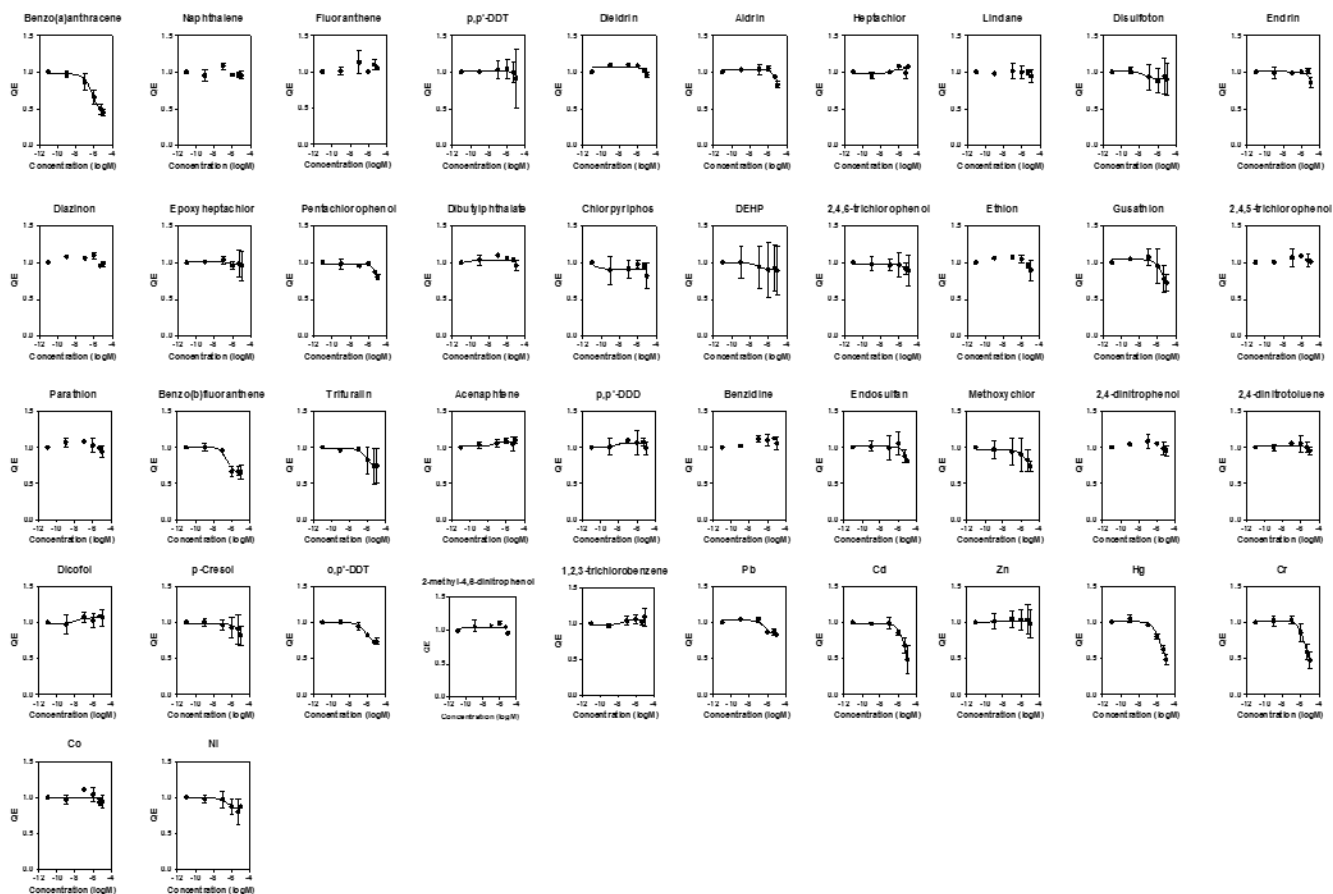


Figure S7. Raw data for the fold quadratic entropy (QE) descriptor in MCF-7 cells treated with the ATSD42 compounds. Average and standard deviation of N=4 is graphed. Summary tables for this figure are in Excel Table S21.

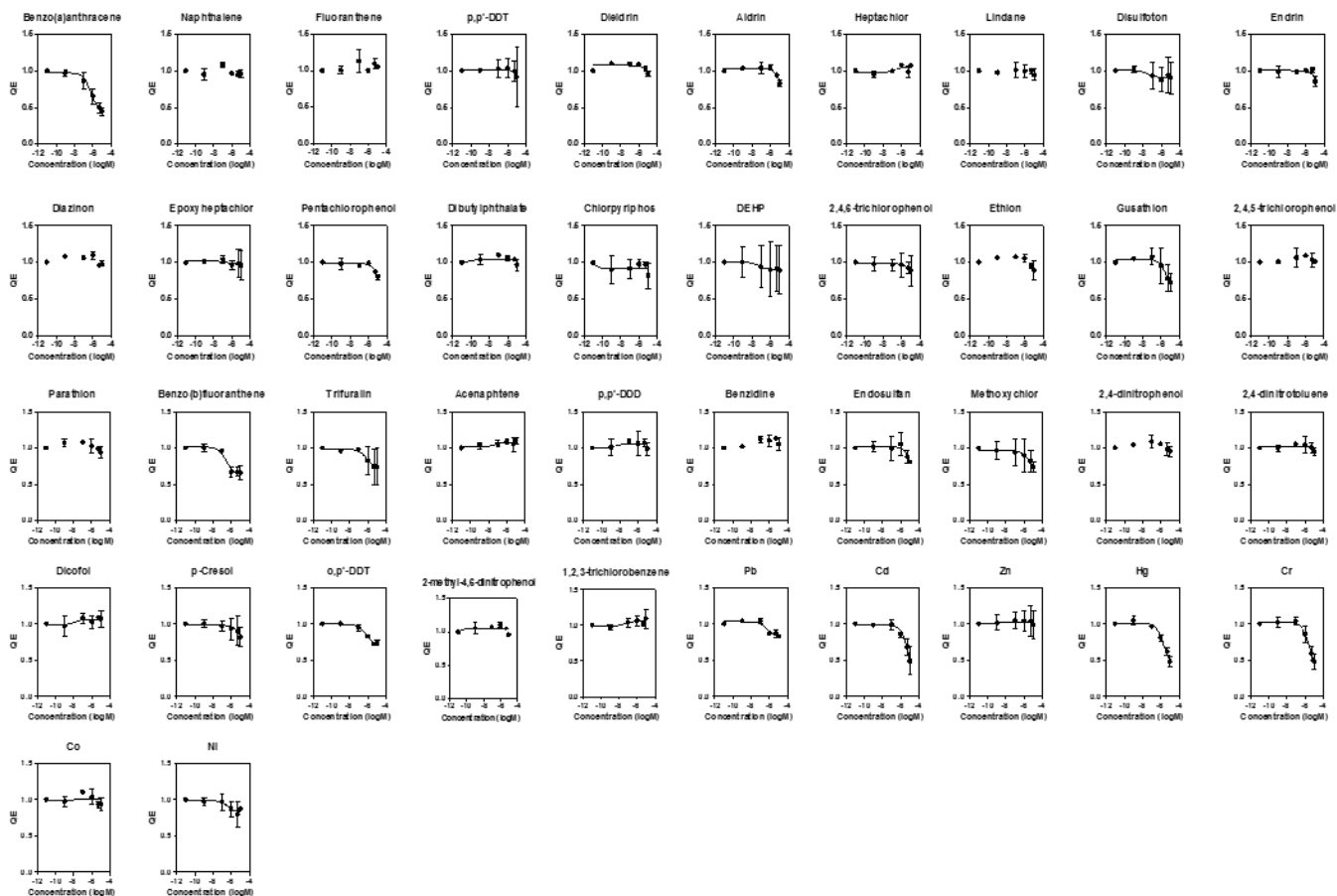


Figure S8. Raw data for the Earth Mover's Distance (EMD) descriptor in MCF-7 cells treated with the ATSDR42 compounds. Average and standard deviation of N=4 is graphed. Summary tables for this figure are in Excel Table S21.

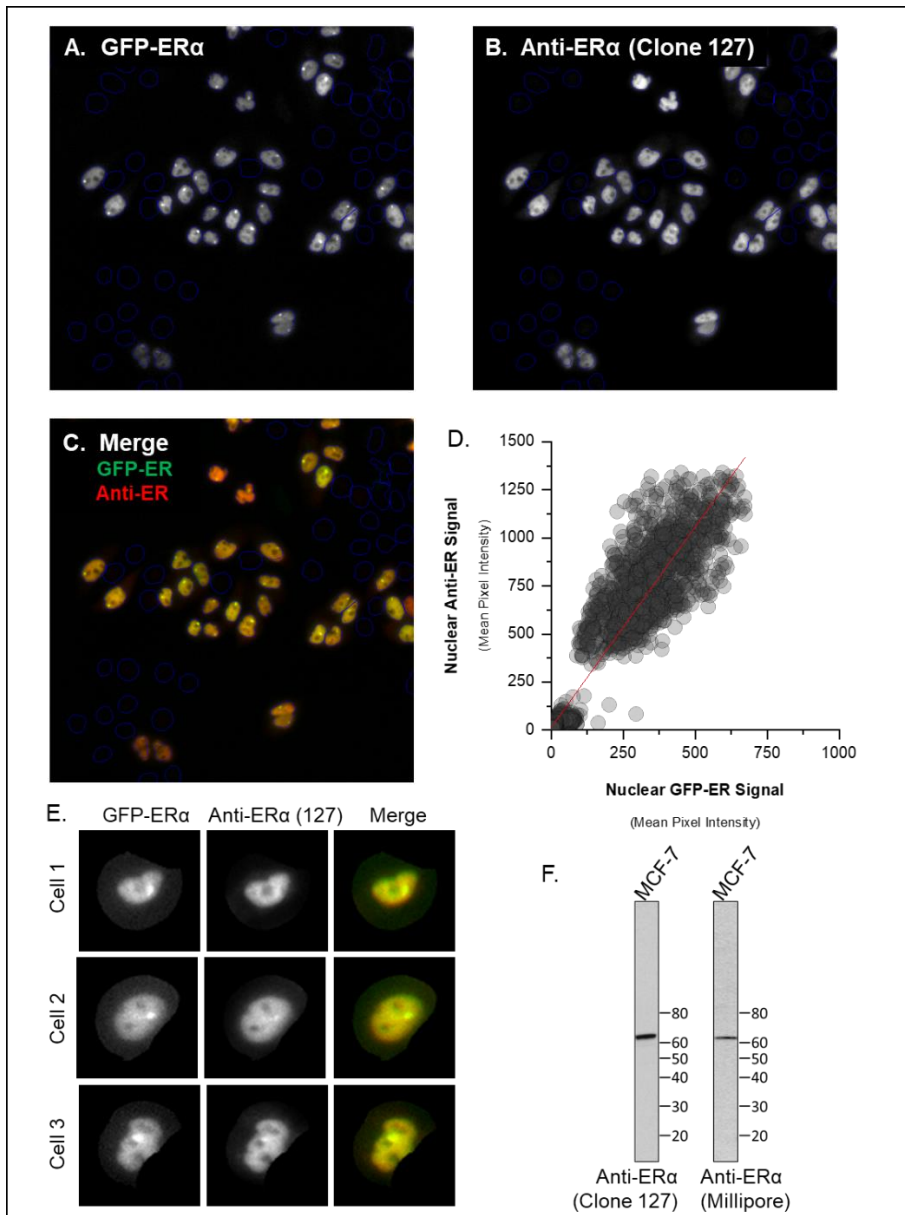


Figure S9. Validation of anti-ER α Clone 127 antibody. An engineered GFP-ER:PRL-HeLa cell line (Ashcroft FJ et al., Gene 2011), that stably expresses GFP-tagged ER α , was treated with 10 nM E2 for 1 hour. Cells were immunolabeled with anti-ER α clone 127 antibody and visualized using an anti-Mouse IgG AlexaFluor 647 secondary. Samples were imaged at 20x/0.75 using an IC200 image cytometer (Vala Sciences). Representative fields of (A) GFP-ER α and (B) anti-ER α clone 127 labeling is shown along with the (C) merged image. Nuclear regions were determined (blue lines) using DAPI staining and nuclear GFP and antibody signal intensity extracted. (D) A scatter-plot comparing single-cell nuclear GFP-ER α and anti-ER α intensity was generated using > 1450 cells. A Pearson's correlation analysis (red line) indicates high correlation (0.97) between the two signals. (E) Representative single cell GFP-ER α , anti-ER α , and merged images are shown which display a high correlation between signals at the sub-nuclear level. (F) Western blot analysis of whole MCF-7 cell lysates probed using anti-ER α clone 127 and anti-ER α clone 60C (Millipore 04-820).

References:

Ashcroft FJ, Newberg JY, Jones ED, Mikic I, Mancini MA. 2011. High content imaging-based assay to classify estrogen receptor- α ligands based on defined mechanistic outcomes. *Gene*. 15;477(1-2):42-52. doi: 10.1016/j.gene.2011.01.009.